

Study of the photoactivation of titania Degussa P25 in ethanol–methanol suspensions using a piezoelectric sensor

R. Trejo-Tzab^a, J.J. Alvarado-Gil^a, P. Quintana^{a,*}, T. López^{b,c}

^a CINVESTAV-Unidad Mérida, Depto. de Física Aplicada, A.P. 73, Cordemex, Mérida, Yuc. México, C.P. 97310, Mexico

^b Universidad Autónoma Metropolitana-Rectoría General, Prol. Canal de Miramontes 3855, Col. Ex-Hda. San Juan de Dios, Tlalpan 14387 México, D.F., Mexico

^c National Institute of Neurology and Neurosurgery “MVS”, Insurgentes Sur 3877, Col. La Fama, México, D.F., C.P. 14269, Mexico

Available online 15 January 2008

Abstract

Photoactivation of titanium oxide Degussa P25 in ethanol–methanol suspensions, with different molar ratios, was monitored in situ using a piezoelectric sensor. The process was studied in a specially designed cell in which the sample can be illuminated by a continuous UV Hg lamp to induce photoactivation. The evolution of the process was followed by sending a modulated red laser beam onto the sample positioned on top of a piezoelectric detector. The output voltage of the sensor is also modulated and its amplitude allows to follow the photoactivation process. In order to control the photoactivation process, the cell was fed with N₂ regulated flux. It is shown that when the sample is illuminated with a UV lamp, the amplitude of the piezoelectric signal falls gradually up to a value that remains constant. The amplitude of the photoactivation, the initial time and the velocity of photoactivation signal of titania are related to ethanol–methanol proportion. The mechanism associated with photoactivation and the role of ethanol–methanol proportion are discussed.

© 2007 Elsevier B.V. All rights reserved.

Keywords: Degussa TiO₂ nanoparticles; UV and visible irradiation; Photoactivation; Piezoelectric detection

1. Introduction

Titanium oxide (TiO₂) is a promising material for photoelectrochemical energy production [1] and photocatalytic applications for oxidative degradation of environmental organic pollutants [2–5], for remediation processes such as water and air purification [6–10], for prevention of stains and sterilization [11–13]. Titania have several advantages as a catalyst, it is an inexpensive material, commercially available in various crystalline forms, non-toxic and photochemically stable. Many approaches to improve titania photocatalytic activity have been tested, and many researchers have pointed out that it is dependent on its phase structure, morphology, crystallinity and surface area [14,15].

Among the three crystalline phases (anatase, rutile and brookite) only anatase and rutile are catalytically active, with a semiconductor band gap located about 3.2 and 3.0 eV, respec-

tively. Many studies have confirmed that anatase presents better photocatalytic properties due to the low recombination rate of its photogenerated electron–holes [15,16]. Moreover, it has been found that the mixture of the two phases of titania was more beneficial for suppressing the recombination of photogenerated electrons and holes, and thus enhance photocatalytic activity [17–21]. The recombination process and the electron–hole formation are favored when OH groups increase.

Most of the literature reports on titania photoactivity mechanisms are related to n-type electrical properties. On the contrary, defect chemistry models are essentially based on the formation of oxygen vacancies and are considered to play an important role in extending the photoactivity of titania into the visible region of the solar spectrum [9,22]. It is also known, that titanium vacancies contribute to p-type conductivity of dense polycrystalline rutile [23,24]. Also, theoretical analysis, as first principles quantum mechanical calculations, has been applied to determine the formation energies of different native defects in anatase, as oxygen and titanium vacancies and interstitials [25]. The results showed that titanium vacancies had the lowest formation energies under oxygen-rich conditions. Furthermore, experimental

* Corresponding author. Tel.: +52 9991242142; fax: +52 9999812917.
E-mail address: pquint@mda.cinvestav.mx (P. Quintana).

evidence for titanium vacancies in TiO₂ sol–gel, determined by Rietveld refinement of powder X-ray diffraction data, proposed that titanium vacancies are compensated for hydroxyl ions incorporated into the structure [26].

Degussa P25, a commercial powder, has been used frequently as a benchmark in titania photocatalysis studies. It has a relatively large surface area, about 53.2 m²/g and an average crystallite size of 25 nm. This powder consists of a mixture of anatase and rutile, with a ratio of 3–4:1 [27], and recent morphology studies by Ohno et al. showed that the particles of these polymorphs exist separately [20]. These authors have also reported that the presence of both phases is important in some photocatalytic reactions where oxygen is used as an electron acceptor [21].

Generally, titania photoactivation has been studied indirectly by exposing different organic compounds and monitoring their degradation rate. Few works have studied the photoreactivity of pure TiO₂ powder by UV–vis, in a slurry-like phenol system [28], water [29] or ethanol [30].

In this work, a new technique is presented to study in situ the photoactivation process of alcohol–titania suspensions, using a piezoelectric sensor [31]. It consists on the simultaneous illumination of the liquid sample by a non-modulated UV lamp and a modulated red laser beam. The UV light induces the photoactivation process changing the optical properties of the sample, which are monitored by a red laser beam light reaching a piezoelectric sensor positioned at the bottom of the container with the suspension. The evolution of the dynamic processes occurring in the sample can be followed with high precision using this procedure. It was shown that the proportion of ethanol-to-methanol mixtures in titania suspensions affects strongly the dynamics of photoactivation.

2. Experimental

2.1. Materials

Commercial titanium oxide in powdered form, Degussa P25, was used. The solutions were prepared in plastic containers by mixing 0.04 g of TiO₂ in 50 mL of solvent. Pure ethanol and methanol, and mixtures in the following molar percentage ratios 17–83, 33–67, 59–41, 82–18, 91–9 (MeOH–EtOH), were studied. After preparation, the solutions were homoge-

nized in an ultrasonic bath during 30 min to obtain a suspension, and kept in a 60 mL plastic container closed with a plastic cap.

2.2. Cell design and measurement technique

The experimental arrangement used in this work is presented in Fig. 1. The sample (4 mL of the suspension) is placed inside of a specially designed glass cylindrical cell (5.7 cm high and 2.5 cm diameter). The bottom of the cell is a ceramic piezoelectric sensor, which is in direct contact with the suspension. To perform the experiments in different atmosphere, the cell is enclosed inside of an upside down bottomless cylindrical glass container (19 cm high and 3.8 cm diameter), closed at the top with a glass slide. A glass pipe, near the top of the container, is connected to a N₂ supplying system with a valve that controls the nitrogen flux inside of the cell during the experiments. The beam of a red laser diode (630 nm) modulated at 15 Hz is sent onto the surface of the sample, in such a way that the light coming from the laser is absorbed or scattered by the sample; therefore, only a fraction of the laser light reaches the sensor. The sensor generates a periodic signal that is measured using a lock-in amplifier (Stanford Research Systems SR850), tuned to detect only the signal at the modulation frequency of the laser. The amplitude of the piezoelectric sensor is registered as a function of time. If any changes in the optical absorption happen, the fraction of light reaching the sensor is modified, which allows to follow the dynamic processes occurring in the sample. In order to induce the photoactivation, the sample is illuminated perpendicularly to the laser beam with a continuous 175 W commercial Hg lamp.

The signal response during the experiments (Fig. 2) is obtained in five stages:

1. Initially to calibrate the system, the experiments were run in air atmosphere during 1000 s, until the signal remains constant.
2. Afterwards the Hg lamp is turned on, the temperature of the sample increases and the piezoelectric detects a decrease of the signal. This situation is maintained until the sensor registers a stable signal (around 3000 s), indicating that the system has reached a constant temperature. The sample does not change in color because the cell is open and the suspension

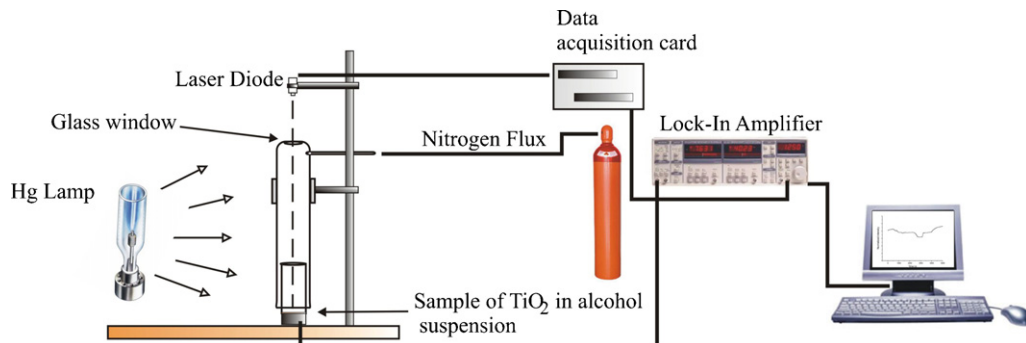


Fig. 1. Sketch of the photoactivation experimental arrangement.

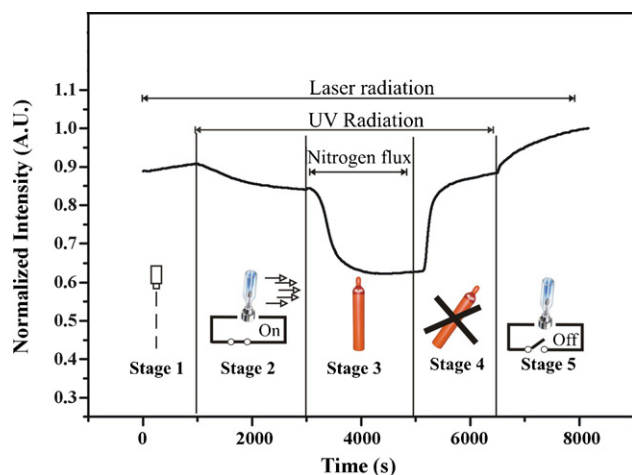


Fig. 2. Typical time scan obtained during the photoactivation and deactivation process, showing the different stages in which the N_2 flux, laser and UV radiation are applied.

is in direct contact with oxygen and the activation cannot be observed.

- In order to observe the photoactivation, the N_2 flux is turned on to expel the O_2 . At the beginning the piezoelectric signal remains stable, but after a few minutes it starts to decrease. This response is related to a change of color of the sample. When it is activated, the white suspension becomes blue and blocks or scatters the red light of the diode laser; the fraction reaching the sensor allows to obtain a precise measurement of the photoactivation process. Afterwards, the signal stabilizes in a time interval that depends on the sample suspension characteristics.
- In this stage the N_2 flux is closed, and the deactivation process is induced, as a consequence the signal amplitude increases rapidly reaching a maximum.
- When the signal of the previous stage stabilizes, the lamp is turned off and the amplitude measured by the detector increases and after some time remains stable. It can be noted that this signal level is higher as compared with the one observed at the first stage. This is due to the evaporation of a small amount of alcohol (0.1 mL) during the experiment.

3. Results and discussion

The piezoelectric amplitude as a function of time, for pure alcohols and mixtures of different concentrations of ethanol–methanol suspensions, are shown in Fig. 3. As can be seen, the general behavior for all samples is very similar; however, the amplitude fall-off and the initial activation time are different.

In order to measure the piezoelectric signal fall-off (S) during stage 3, a sigmoidal fitting was performed [32] using the following equation in function time, t :

$$S = A_2 + \frac{A_1 - A_2}{1 + (t/t_0)^p} \quad (1)$$

where A_1 and A_2 are the highest and lowest amplitude values of the sigmoidal curve (Fig. 3). When $t \gg 1$, $|A_1 - A_2|$ is the

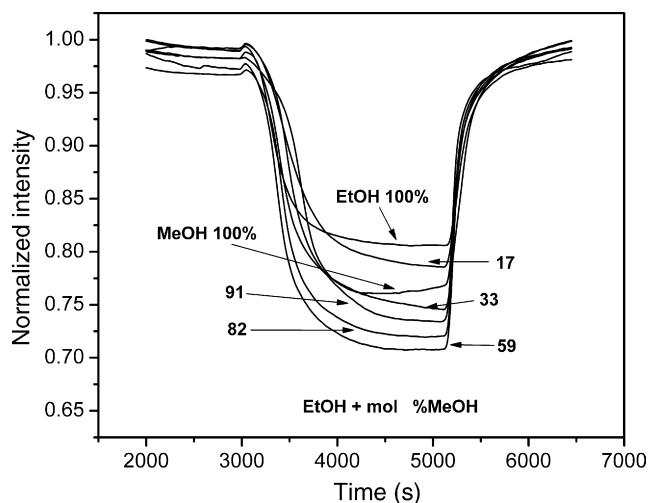


Fig. 3. Results for the normalized amplitude as a function of time for samples of titania suspensions of pure EtOH and MeOH, and mixtures of ethanol–methanol.

total decrement of the sigmoidal; t_0 is the sigmoidal inflexion point that measures the time at which the process is in the middle, and p determines the rate at which the signal (S) decreases. The piezoelectric amplitude $|A_1 - A_2|$ due to the photoactivation (Fig. 4) shows an increase with methanol content, reaching a maximum around 60 mol% and diminishing afterwards.

On the contrary, in order to analyze the velocity of the process, the time derivative of the signal was obtained (Fig. 5); the minimum point determines the maximum speed at which the photoactivation process occurs. This value increases slightly for a methanol concentration of around 60 mol%.

The velocity presents a Lorentzian-like behavior, the width of the transition and the height of the peak can be obtained using the equation:

$$\frac{dS}{dt} = \frac{dS_i}{dt} + \frac{2A}{\pi} \frac{w}{4(t - t_0)^2 + w^2} \quad (2)$$

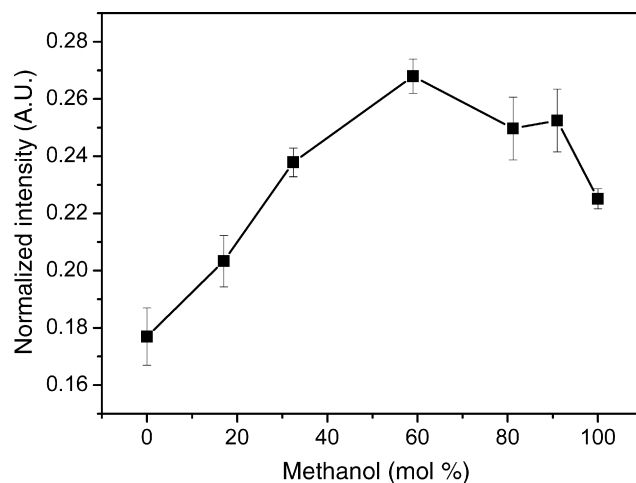


Fig. 4. Normalized photoactivation amplitude (in arbitrary units) as a function of methanol concentration.

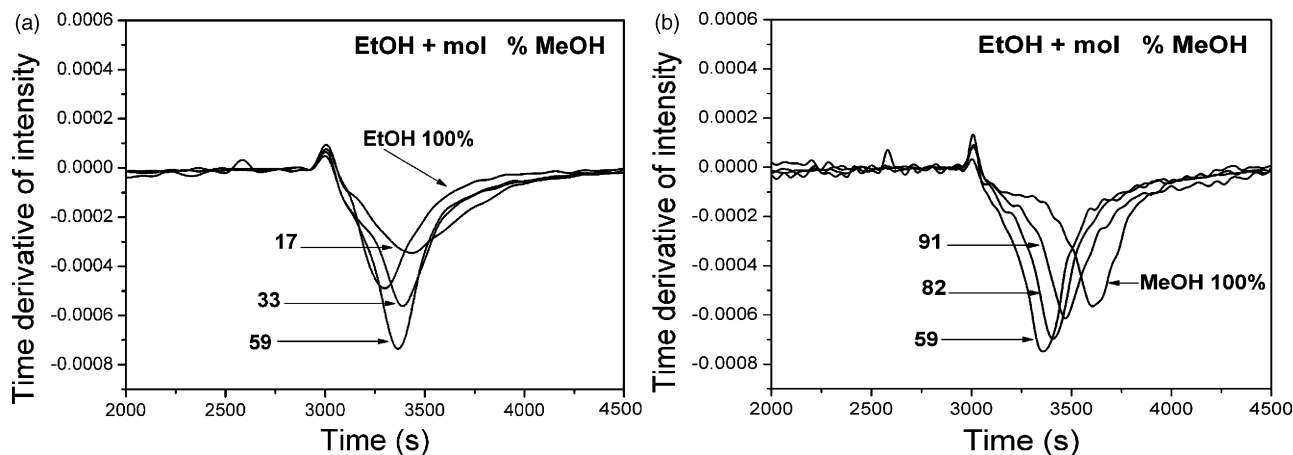


Fig. 5. Time derivative (in arbitrary units) of the piezoelectric amplitude for photoactivation as a function of time: (a) 100% EtOH and 17, 33, 59 mol% of MeOH and (b) 59, 82, 91 and 100% MeOH.

where dS_i/dt is the velocity far from the time t_0 , at which the time derivative reaches its maximum. A and w are the area and the half width height of the peak, respectively.

Additionally, the effective time at which the photoactivation process starts is obtained from the fitting parameters in the following form:

$$t_i = t_0 - \frac{w}{2} \quad (3)$$

and measures the time at which the piezoelectric signal starts to change due to the photoactivation process.

The initial time for photoactivation (t_i) shows an increase when MeOH content grows (Fig. 6). For concentrations under 60 mol%, t_i grows slowly and above this concentration a strong increment is observed.

In order to explain our experimental results, it is important to mention the main reactions involved in the photoactivation process [33–35]. Initially, the UV light reaching the titania suspension induces the generation of hole–electron pairs:

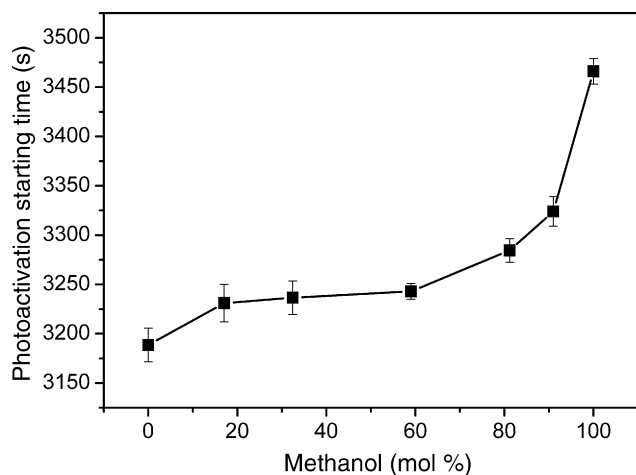


Fig. 6. Behavior of the initial activation time as a function of methanol concentration.

If the charge recombination is prevented or delayed, titanium is reduced by the electrons



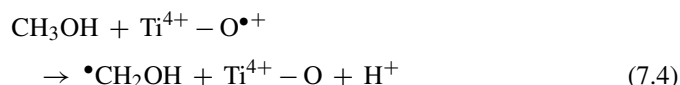
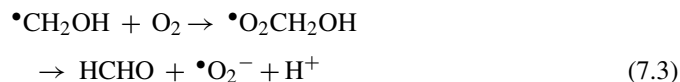
As a consequence, titania becomes blue [36,37] and the piezoelectric signal falls corresponding to stage 3 in Fig. 2 and the time interval from 3000 to 5000 s in Fig. 3. The total decrease of the signal in this stage, can be parametrized by the factor $|A_1 - A_2|$ (Eq. (1)) that measures how strong is the activation process. On the contrary, the time at which this decrement is observable corresponds to the initial time (t_i).

In alcohol suspensions, electrons can also be attached to oxygen in the form [33–35],



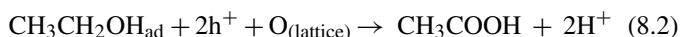
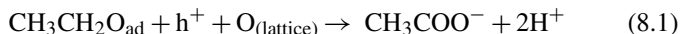
This mechanism goes against the formation of Ti^{3+} , and therefore could induce the sample to become white.

In the case of methanol, the photogenerated holes interact with the hydroxyl ions and lead to the following processes [38,39]:



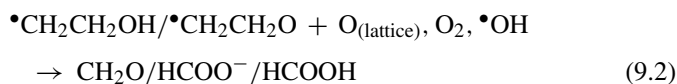
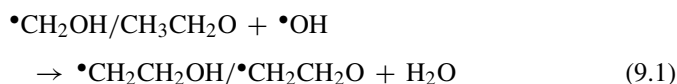
According to these results, methanol functions as a hole scavenger and therefore favors titania photoactivity [40].

For pure ethanol, Eq. (7.1) is also valid; nevertheless, instead of Eqs. (7.2)–(7.4), we have the following reactions [33]:



In this case, the hole trapping mechanisms are not as efficient as in methanol (Eqs. (7.1)–(7.4)) [33]; therefore, titania photoactivation is lower in ethanol suspension than in methanol one. This effect can be observed in Figs. 3 and 4, in which it is shown that the photoactivity of titania in methanol is 28% higher than in ethanol.

However, in a titania methanol–ethanol mixture, the mechanisms described in Eqs. (7) and (8) are also present, but in this case the interaction with $\bullet\text{OH}$ radicals could be enhanced by ethanol oxidation [33]:



The synergy of both mechanisms in ethanol–methanol mixture, is clearly observed in Fig. 4, where the maximum intensity is around 60 mol% of methanol. This behavior can be interpreted as a higher hole consumption in the mixture than when pure alcohols are used, diminishing the recombination process of the hole–electron pairs and enhancing Ti^{4+} to Ti^{3+} reduction.

For concentrations above 60 mol% MeOH, photoactivation decreases since the hole interaction does not proceed by the mechanisms shown in Eq. (8), which is only valid for high ethanol concentrations [33]. At this stage, the hole excess increases the charge recombination and diminishes the formation of Ti^{3+} .

On the contrary, the initial time (Fig. 6) slowly grows up to 60 mol% MeOH, since the photogenerated holes are more easily trapped by ethanol than by methanol (see Eqs. (7) and (8)). At higher methanol content, the slower hole scavenging effect is dominant (Eq. (7)) delaying the starting time of the photoactivation process, and therefore the initial time increases steeply. The delay in the initial time could be related to the mechanisms presented in Eq. (9), where the activation process is controlled by $\bullet\text{OH}$ radicals. A higher number of radicals (which is increased at higher methanol content) produces a larger delay in the initial time.

4. Conclusions

The photoactivation of titanium oxide Degussa P25 in ethanol–methanol suspensions, with different molar ratios, was monitored at real time using a piezoelectric sensor. The photoactivation process generates a gradual decrement in the piezoelectric signal until it remains constant. In contrast, deactivation is observed as a gradual increase reaching its stabilization after a time interval. The analysis of the experimental data of the activation kinetics provides the parameters corresponding to the total change of the amplitude, initial time and velocity of the different stages of the process. The photoactivation pro-

cess amplitude increases with methanol content and reaches a maximum around 60 mol% MeOH. For higher concentrations of methanol, the signal amplitude falls down gradually up to pure methanol value.

The initial time increases slowly when the methanol proportion grows, however above 60 mol%, it increases steeply. The observed results can be explained in terms of the combined effect of ethanol and methanol. Ethanol favors the fast consumption of the photogenerated holes, on the contrary, methanol prevents the recombination of electron–hole pairs, acting as a photoactivation controller. These results can be useful in providing information in choosing the appropriate mixtures of alcohols for specific applications of photocatalytic reactions.

Acknowledgements

The authors wish to thank M.C. J. Bante and M.C. D.H. Aguilar for technical assistance.

References

- [1] J. Nowotny, C.C. Sorrell, T. Bak, L.R. Sheppard, *Sol. Energy* 78 (2005) 593–602.
- [2] G. Martra, S. Coluccia, L. Marchese, V. Augugliaro, V. Loddo, L. Palmisano, M. Schiavello, *Catal. Today* 53 (1999) 695–702.
- [3] F. Bertinchamps, M. Treinen, P. Eloy, A.-M. Dos Santos, M.M. Mestdagh, E.M. Gaigneaux, *Appl. Catal. B* 70 (2007) 360–369.
- [4] A. Syoufian, O.H. Satriya, K. Nakashima, *Catal. Commun.* 8 (2007) 755–759.
- [5] G. Palmisano, M. Addamo, V. Augugliaro, T. Caronna, A. Di Paola, E. Garcia Lopez, V. Loddo, G. Marci, L. Palmisano, M. Schiavello, *Catal. Today* 122 (2007) 118–127.
- [6] G.-M. Zuo, Z.-X. Cheng, G.-W. Li, W.-P. Shi, T. Miao, *Chem. Eng. J.* 128 (2007) 135–140.
- [7] K. Azrague, P. Aimar, F. Benoit-Marquie, M.T. Maurette, *Appl. Catal. B* 72 (2007) 197–204.
- [8] A.M.T. Silva, E. Nouli, N.P. Xekoukoulotakis, D. Mantzavinos, *Appl. Catal. B* 73 (2007) 11–22.
- [9] I. Nakamura, N. Negishi, S. Kutsuna, T. Ihara, S. Sugihara, K. Takeuchi, *J. Mol. Catal. A* 161 (2000) 205–212.
- [10] M. Higarashi, W. Jardim, *Catal. Today* 76 (2001) 201–207.
- [11] K. Rajeshwar, C.R. Chenthamarakshan, S. Goeringer, M. Pjucic, *Pure Appl. Chem.* 73 (2001) 1849–1860.
- [12] L.K. Adams, D.Y. Lyon, P.J.J. Alvarez, *Water Res.* 40 (2006) 3527–3532.
- [13] P.A. Christensen, T.P. Curtis, T.A. Egerton, S.A.M. Kosa, J.R. Tinlin, *Appl. Catal. B* 41 (2003) 371–386.
- [14] Y. Li, T. White, S.H. Lim, *Rev. Adv. Mater. Sci.* 5 (2003) 211–215.
- [15] J. Yu, J.C. Yu, M.K.-P. Leung, W. Ho, B. Cheng, X. Zhao, J. Zhao, *J. Catal.* 217 (2003) 69–78.
- [16] H. Bieber, P. Gilliot, M. Gallart, N. Keller, V. Keller, S. Begin-Colin, C. Pighini, N. Millot, *Catal. Today* 122 (2007) 101–108.
- [17] B. Sun, A.V. Vorontsov, P.G. Smirniotis, *Langmuir* 19 (2003) 3151–3156.
- [18] B. Sun, P.G. Smirniotis, *Catal. Today* 88 (2003) 49–59.
- [19] M. Yan, F. Chen, J. Shang, M. Anpo, *J. Phys. Chem. B* 109 (2005) 8673–8678.
- [20] T. Ohno, K. Sarukawa, K. Tokieda, M. Matsumura, *J. Catal.* 203 (2001) 82–86.
- [21] T. Ohno, K. Sarukawa, M. Matsumura, *J. Phys. Chem. B* 105 (2001) 2417–2420.
- [22] I.N. Martyanov, S. Uma, S. Rodriguez, K.J. Klabunde, *Chem. Commun.* 21 (2004) 2476–2477.
- [23] T. Bak, T. Burg, S.-J.L. Kang, J. Nowotny, M. Rekas, L. Sheppard, C.C. Sorrell, E.R. Vance, Y. Yoshida, M. Yamawaki, *J. Phys. Chem. Solids* 64 (2003) 1089–1095.

- [24] D.S. Kim, S.-Y. Kwak, *Appl. Catal. A* 323 (2007) 110–118.
- [25] S.N. Phattalung, M.F. Smith, K. Kim, M.-H. Du, S.-H. Wei, S.B. Zhang, S. Limpijummong, *Phys. Rev. B* 73 (2006) 125205–125216.
- [26] J.A. Wang, R. Limas-Ballesteros, T. Lopez, A. Moreno, R. Gomez, O. Novaro, X. Bokhimi, *J. Phys. Chem. B* 105 (2001) 9692–9698.
- [27] A.K. Datye, G. Riegel, J.R. Bolton, M. Huang, M.R. Prairie, *J. Solid State Chem.* 115 (1995) 236–239.
- [28] U.C.B. Almquist, P. Biswas, *J. Catal.* 212 (2002) 145–156.
- [29] C.-C. Wang, Z. Zhang, J.Y. Ying, *Nanostruct. Mater.* 9 (1997) 583–586.
- [30] A.R. Caamal-Parra, R.A. Medina-Esquivel, T. Lopez, J.J. Alvarado-Gil, P. Quintana, *J. Non-Cryst. Sol.* 353 (2007) 971–973.
- [31] D. Almond, P. Patel, *Photothermal Science and Techniques*, Chapman and Hall, Malabar, Florida, 1996.
- [32] G. Aguirre, G. Arriola, J. Gómez-Hernández, T. López, M. Picquart, D.H. Aguilar, P. Quintana, J.J. Alvarado-Gil, *Thermochim. Acta* 421 (2004) 211–215.
- [33] Z. Yu, S.C. Chuang, *J. Catal.* 246 (2007) 118–126.
- [34] J. Marugan, D. Hufschmidt, M.J. Lopez-Muñoz, V. Selzer, D. Bahnemann, *J. Appl. Catal. B: Environ.* 62 (2006) 201–207.
- [35] L. Sun, J.R. Bolton, *J. Phys. Chem.* 100 (1996) 4127–4134.
- [36] Z. Zhang, P.A. Maggard, *J. Photochem. Photobiol. A: Chem.* 186 (2007) 8–13.
- [37] W. Kongsuebchart, P. Praserthdam, J. Panpranot, A. Sirisuk, P. Supphasrirongjaroen, C. Satayaprasert, *J. Cryst. Growth* 297 (2006) 234–238.
- [38] J. Marugán, D. Hufschmidt, M.J. Lopez-Muñoz, V. Selzer, D. Bahnemann, *J. Appl. Catal. B: Environ.* 62 (2006) 201–207.
- [39] C. Wang, J. Rabani, D.W. Bahnemann, J.K. Dohrmann, *J. Photochem. Photobiol. A: Chem.* 148 (2002) 169–176.
- [40] D.C. Hurum, A.G. Agrios, K.A. Gray, T. Rajh, M.C. Thurnauer, *J. Phys. Chem. B* 107 (2003) 4545–4549.